

**United States
Department of
Agriculture**

**Natural Resources
Conservation
Service**

**100 Campus Boulevard
Suite 200
Newtown Square, PA 19087-4585**

Subject: Archaeology -- Geophysical Assistance

Date: April 6, 2007

To: Jason Lott
Superintendent
USDI-National Park Service
Casa Grande Ruins National Monument
1100 Ruins Drive
Coolidge, AZ 85228

Purpose:

Ground-penetrating radar (GPR) and electromagnetic induction (EMI) surveys were conducted at Casa Grande Ruins National Monument in an attempt to nondestructively identify and map buried, prehistoric features dating to prehistoric Hohokam occupation (approximately 300 to 1500 AD).

Principal Participants:

Aron Adams, Archaeology Technician, USDI-NPS, Casa Grande Ruins National Monument, Coolidge, AZ
Rebecca Carr, Chief of Cultural Resources, USDI-NPS, Casa Grande Ruins National Monument,
Matthew Bilsbarrow, Archeologist, Arizona State Historic Preservation Office, Phoenix, AZ
Joann Medley, Archeologist, Arizona State Historic Preservation Office, Phoenix, AZ
Ronald Beckwith, Archeologist, Western Archeological Conservation Center, Tucson, AZ
Jim Doolittle, Research Soil Scientist, USDA-NRCS-NSSC, Newtown Square, PA
Eric Drummond, GIS Analysis, USDI-NPS-IRGR, Lakewood, CO
Nelda Greager, Volunteer, USDI-NPS, Casa Grande Ruins National Monument, Coolidge, AZ
Jim Hevelone, Volunteer, USDI-NPS, Casa Grande Ruins National Monument, Coolidge, AZ
Sandy Hevelone, Volunteer, USDI-NPS, Casa Grande Ruins National Monument, Coolidge, AZ
Gerald Kelso, Archaeologist, USDA-NRCS, Phoenix, AZ
Karen Munroe, Research Assistant, Dept. Wildlife & Fisheries Resources, University of Arizona, Tucson, AZ

Activities:

All field activities were completed during the period of 12 and 16 March 2007.

Summary:

1. At Casa Grande Ruins National Monument, in areas of Coolidge soils, sufficient penetration depths were achieved with GPR to profile most archaeological features. Both the 200 and 400 MHz antenna provided comparable penetration depths (about 1 m). However, the higher resolution of the 400 MHz antenna is more suitable for archaeological investigations.
2. In general, buried caliche walls do not sufficiently contrast with the surrounding soil materials in dielectric properties to produce strong and easily identifiable reflections on radar records. Various data processing techniques and display options failed to make these features discernible on 2D radar records and 3D pseudo-images. Where known buried walls were traversed with the radar, reflections were indistinct and did not produced laterally coherent reflection patterns.

3. Wetter soil conditions masked reflections from buried, prehistoric caliche walls that were observed under dry conditions.
4. GPR and advanced data processing techniques can be used to map the burrows of round-tailed ground squirrels. While adequate radar data were obtained with a 400 MHz antenna, the use of a higher frequency antenna (900 MHz) should be explored.
5. Electromagnetic induction is can be used to identify and map midden mounds. As a rapid reconnaissance tool, EMI can be effectively used to map these features within the National Monument, assess their occurrence and distribution in other areas, where they are less obvious or have been leveled for agriculture.

It was my pleasure to work at Casa Grande National Monument and to be of involved in this project.

With kind regards,

James A. Doolittle
Research Soil Scientist
National Soil Survey Center

cc:

- B. Ahrens, Director, USDA-NRCS, National Soil Survey Center, Federal Building, Room 152, 100 Centennial Mall North, Lincoln, NE 68508-3866
- P. Camp, State Soil Scientist/MLRA Office Leader, USDA-NRCS, 230 N. First Avenue, Suite 509, Phoenix, AZ 85003-1733
- R. Carr, Archaeologist, USDI-National Park Service, Casa Grande Ruins National Monument, 1100 Ruins Drive, Coolidge, AZ 85228
- M. Golden, Director of Soils Survey Division, USDA-NRCS, Room 4250 South Building, 14th & Independence Ave. SW, Washington, DC 20250
- D. Hammer, National Leader, Soil Investigation Staff, USDA-NRCS, National Soil Survey Center, Federal Building, Room 152, 100 Centennial Mall North, Lincoln, NE 68508-3866
- K. Munroe, Research Assistant, University of Arizona, Dept. Wildlife & Fisheries Resources, 104 Biosciences East Bldg., Tucson, AZ 85721

Background:

Casa Grande is Spanish for “Big House.” In 1694, this name was applied by Father Eusebio Francisco Kino to remnants of a large, pre-Columbian, four story structure located within the Phoenix Basin near present-day Coolidge, Arizona. Typically, these people lived in permanent settlement consisting of pit houses in the earlier periods, walled compounds in the later periods. The Casa Grande Great House is a large earthen building that is best known for its engineering success and good preservation. The size and preservation of this Great House structure indicates a high level of social organization during the Classic Period of Hohokam culture. The building was constructed of caliche, a harden mixture of local soil materials enriched with calcium carbonate. Casa Grande was believed to be constructed during the Classic Period of Hohokam occupation (about 1200 to 1500 AD). In 1892, President Benjamin Harrison proclaimed *Casa Grande* as the Nations first archaeological preserve. In 1918, President Woodrow Wilson redesignated *Casa Grande* as a national monument.

Casa Grande Ruins National Park preserves 61 known archeological sites within its boundaries. No site within the park has been fully excavated and archaeological investigations have been limited. The monument is visited by as many as 1,000 visitors per day, and the resulting foot traffic has caused substantial erosion in some areas. This is especially true within *Compound A*, which contains *Casa Grande*. Within the park, a majority of the structural walls remain buried. Some of the original walls are being impacted by foot traffic and exposed to erosional processes. As a major part of this study, ground-penetrating radar (GPR) surveys were conducted to help identify and map the locations of subsurface architectural features. Knowledge of these subsurface features will aid the preservation, management and interpretation of this irreplaceable resource.

Ground-penetrating radar has been widely used as a rapid, relatively inexpensive geophysical method for identifying subsurface archaeological features. As GPR surveys are nondestructive, they are frequently used to obtain subsurface information at archaeological sites without the disturbance of historic structures. In these archaeological investigations, GPR has been used to locate buried structures, obtain information on the type and condition of structural materials, and identify different constructional layers (Evangelista et al., 2002; Jol et al., 2002; Colla and Maierhofer, 2000; Pérez Gracia et al., 2000). Ground-penetrating radar has been used to identify and locate buried artifacts from prehistoric, indigenous cultures (Berard and Maillol, 2007; da Silva Cezar et al., 2001; Whiting et al., 2001a & 2001b). In most of these studies, the small size of some buried artifacts (bones, pottery, and urns), the low dielectric contrast between the artifact and the host soil materials, and the relatively high electrical conductivity of the soil created unique challenges and limitations to GPR surveys. However, in some studies, under more suitable soil conditions, results of GPR surveys have been impressive. Whiting et al. (2001a & 2001b), working in areas of dry, clean quartz sands, identified remnants (including postholes) of a prehistoric house structure associated with the Amerindian culture in Barbados.

Ground-penetrating radar has been frequently used to support archaeological investigations in the American Southwest (Conyers and Osburn, 2006; Conyers and Cameron, 1998; Baker et al., 1997; Sternberg and McGill, 1995; Vickers et al., 1976). Here, many prehistoric archaeological features are only recognizable by the scatter of artifacts on the soil surface or the presences of shallow depressions (Conyers and Cameron, 1998). Conyers and Osburn (2006) used GPR to distinguished stone walls and compacted earthen floors of buried kivas associated with the Chaco culture in southeastern Utah. In their investigations, detailed (50 cm interval) parallel GPR traverses were used to reveal small rooms and pit structures in several depressions, which were covered by sandy aeolian deposits. Baker et al. (1997) used GPR at the Elden Pueblo Ruins (Flagstaff, Arizona), to identify and locate buried stone wall structures, rock lined pits, and grave sites. Sternberg and McGill (1995) use GPR to investigate a series of Hohokam compounds in southern Arizona. Though the basin-filled sediments were highly attenuating and depth restricting to GPR, Sternberg and McGill (1995) use a relatively high frequency, 500 MHz antenna to image buried adobe walls and pits. At Casa Grande National Monument, they profiled a Hohokam canal system (northwest corner of park) and a buried structure south of the *Clan House*. A more detailed GPR investigation was recommended to map the actual floor plan of this structure. At a Hohokam site in the Tucson Basin, Conyer and Cameron (1998) used GPR and advanced processing techniques to identify the floors of buried pit structures.

In recent years, a number of processing techniques have become available to “*cleanup*” radar data and improve

interpretations. As noted by Conyers (2006) computer processing “compares digital [radar] data in a way the human brain cannot, producing complex databases, profiles, and maps of spatial variations of both distinct and subtle reflections.” Different processing techniques are often used to meet the specific characteristics of the buried archaeological features (e.g., size, construction, depth). Typically, these processing techniques are adjusted to site conditions and the quality of the radar reflections (Conyers and Cameron, 1998).

In many instances, resource constraints have limited the use of GPR to two-dimensional (2D) data acquisition. A weakness of 2D GPR interpretations is that targets are often indistinct and separated by distances that involve the risks of incorrect geometrical reconstructions and/or interpretations (Lualdi et al., 2006). In recent years, three-dimensional (3D) GPR techniques have been used to image subtle or low amplitude reflectors, which are not easily identifiable on 2D radar records. Because 3D radar surveys can provide more complete information concerning the presence and geometry of subsurface features, this technique has been used extensively to identify both modern and historic subsurface structural features (Evangelista et al., 2002; Utsi and Alani, 2002; Whiting et al., 2001a & 2001b; Leckebusch, 2000; Nobes and Lintott, 2000; Pipan et al., 1999), burials and tombs (Conyers, 2006; Utsi, 2006). In these studies, buried archaeological features were identified by their depth, spatial shape (linearity), extent, and reflected signal amplitudes.

The use of digital signals and sophisticated signal-processing software, have enabled signal enhancement and improved pattern-recognition in some radar surveys. In recent years, a sophisticated type of GPR data manipulation, known as *amplitude slice-map analysis*, has been used in archaeological investigations (Conyers and Goodman, 1997). In this procedure, amplitude differences within the 3D image are analyzed in "time-slices" to isolate differences within specific time (i.e., depth) intervals (Conyers and Goodman, 1997). Time-sliced data are created by averaging the reflected radar energy horizontally between adjoining sets of parallel radar traverses within a specified time window. The resulting pseudo-image shows the spatial distribution of reflected signal amplitudes, which are interpreted as representing lateral changes in soil properties or the presence of subsurface features.

Regardless of the sophistication of the radar unit and processing techniques, limitations to GPR surveys exist. Electrically conductive soils rapidly attenuate the radar signal and limit penetration depths. Shallow penetration depths often plague GPR surveys in areas of highly conductive soils. This is particular true in clayey, sodic or saline soils. Sternberg and McGill (1995) reported penetration depths of less than 1 m through basin-filled sediments in southern Arizona. Sternberg and McGill's observations are slightly more favorable than the potential rating provided for the soils of Casa Grande Ruins National Monument in the USDA soil databases and the Arizona State GPR Soil Suitability Maps (<http://soils.usda.gov/>).

Densely vegetated areas and uneven ground surfaces have a negative impact on GPR surveys (Conyers and Cameron, 1998). This is due to variations in antenna coupling and antenna orientation with changes in vegetal cover and slope. Significant improvements in noise reduction and data interpretation are achieved where sites are relatively flat and non-vegetated (Evangelista et al., 2002). Restrictions are often imposed on radar surveys and interpretations because of the size and complexity of archaeological sites (Dabas et al., 2000). Accessible sites may be too small or cluttered to conduct a GPR surveys, and interpretations can be limited by the incapacity to discriminate natural, historic, and modern subsurface features from one another. If a survey area is densely cluttered with construction rubble and debris, chaotic radar reflection patterns can mask the extension of buried floors and walls (Bevan et al., 1984).

GPR interpretations of buried archaeological structures are often facilitated by the synergistic use of other geophysical techniques such as electromagnetic induction, resistivity, magnetometer, and magnetic gradiometry (Evangelista et al., 2002; Moorman et al., 2002; Utsi and Alani, 2002; Colla and Maierhofer, 2000; Dabas et al., 2000; Nobes and Lintott, 2000; Sambuelli et al., 1999; Imai et al, 1987). Electromagnetic induction (EMI) is often used to rapidly map and characterize relatively large areas. Electromagnetic induction has been used as a fast, easy to use, reconnaissance tool in archaeological investigations. This tool has been used to map tombs and burial chambers, borrow pits, middens, and mounds (Dalan and Bevan, 2002; Dalan, 1990; Frohlich and Lancaster, 1986; Bevan, 1983). Bevan (2000) reported the use of EMI at Casa Grande Ruins National

Monument and the measurement of higher apparent conductivity over possible middens and canals. In addition, Bevan (2000) used resistivity to locate prehistoric buried middens, adobe walls, and canals at Fort Lowell and Casa Grande Ruins National Monument.

Through a hierarchical approach, EMI and GPR methods are often combined to support archaeological investigations. In this approach, EMI provides a rapid, lower resolution overview of a larger area. This allows the use of the higher resolution GPR to be focused onto smaller target areas. As complementary methods, these geophysical tools can provide a more complete evaluation of buried archaeological features. At many sites, the heterogeneity of the earthen materials, the limited contrast between soil and cultural features, and low signal to noise ratios make multi-method acquisition and data comparison necessary (Sambuelli et al., 1999).

Equipment:

The radar unit is the TerraSIRch Subsurface Interface Radar (SIR) System-3000, manufactured by Geophysical Survey Systems, Inc. (North Salem, New Hampshire).¹ The SIR System-3000 weighs about 9 lbs and is backpack portable. With an antenna, this system requires two people to operate. The 200, 400, and 900 MHz antennas were used in this investigation. However, the 900 MHz antenna malfunctioned and produced high levels of background noise and no meaningful signal. This antenna was returned to the manufacturer for repairs and maintenance. The 200 and 400 MHz antennas provided similar penetration depths in the soils at Casa Grande Ruins National Monument. In electrically conductive soils, radar energy is effectively dissipated at relatively shallow soil depths regardless of antenna frequency (Lucius and Powers, 1997). The higher-frequency, 400 MHz antenna provided superior resolution and became the antenna of choice for the GPR investigations discussed in this report.

Radar records contained in this report were processed with the RADAN for Windows (version 5.0) software program (Geophysical Survey Systems, Inc).¹ Each radar record was submitted to the following processing procedures: setting the initial pulse to time zero, color transformation, marker editing, distance normalization, horizontal stacking, and background removal. For each grid site, the processed radar records were combined into a three-dimensional pseudo-image using the 3D QuickDraw for RADAN Windows NT software (Geophysical Survey Systems, Inc).¹ Initially, processed radar pseudo-images were migrated and the gain adjusted for display purposes. However, migration did not improve interpretations and many of the pseudo-images shown in this report represent non-migrated data. Once processed, arbitrary cross sections and time-slices were viewed and selected images attached to this report.

Electromagnetic induction surveys of two compounds were conducted with an EM38 meter (Geonics Limited, Mississauga, Ontario).¹ This meter weighs about 1.4 kg (3.1 lbs) and needs only one person to operate. No ground contact is required with this instrument. The EM38 meter has a 1-m intercoil spacing and operates at a frequency of 14,600 Hz. When placed on the soil surface, it has effective penetration depths of about 0.75 m and 1.5 m in the horizontal and vertical dipole orientation, respectively (Geonics Limited, 1998).

Geonics' DAS70 Data Acquisition System was used with the EM38 meter to record and store both apparent conductivity (EC_a) and position data.¹ The acquisition system consists of the EM38 meter, an Allegro CX field computer (Juniper Systems, North Logan, UT), and a Garmin Global Positioning System (GPS) Map 76 receiver (with CSI Radio Beacon receiver, antenna, and accessories that are fitted into a backpack)(Olathe, KS).² When attached to the acquisition system, the EM38 meter is keypad operated and measurements can be automatically triggered. The NAV38 and Trackmaker38 software programs developed by Geomar Software Inc. (Mississauga, Ontario) were used to record, store, and process EC_a and GPS data.²

To help summarize the results of the EMI surveys, SURFER for Windows, version 8.0 (Golden Software, Inc., Golden, CO), was used to construct simulations of EC_a data.¹ Grids of EC_a data shown in this report were created using kriging methods with an octant search.

¹ Manufacturer's names are provided for specific information; use does not constitute endorsement.

Survey Procedures:

To collect data required for the construction of 3D GPR pseudo-images, survey grids were established at each site. Each grid was constructed using two equal length and parallel lines, which formed the opposing sides of a rectangular area. Along these parallel axes, survey flags were inserted into the ground at a uniform spacing of 25, 50 or 100 cm (grid interval), and a reference line was stretched between matching survey flags on opposing sides of the grid using a distance-graduated rope (see Figure 1). GPR traverses were conducted along this reference line. An antenna was towed on the soil surface along the graduated rope and, as it passed each 100-cm graduations, a mark was impressed on the radar record. Following data collection, the reference line was sequentially displaced (a uniform distance of 25, 50 or 100 cm) to the next pair of survey flags to repeat the process.

Random walk or *wild-cat* EMI surveys were conducted across Compounds C and IX with the EM38 meter and the DAS70 Data Acquisition System. The EM38 meter was operated in the deeper-sensing (0 to 1.5 m) vertical dipole orientation. The EM38 meter was held about 3 cm (about 1 inch) above the ground surface and orientated with its long axis parallel to the direction of traverse. Surveys were completed by walking at a uniform pace, in a random pattern across each compound. Only quadrature phase data were recorded. Data were expressed as values of apparent conductivity (EC_a) in milliSiemens/meter (mS/m). The EM38 was operated in the continuous mode (measurements recorded at 1-sec intervals). Using the NAV38 program, both GPS and EC_a data were simultaneously recorded on the field computer. The EC_a measurements discussed in this report were not temperature corrected.

Survey Site:



Figure 1. A marked reference line (foreground) is stretched between two parallel, flagged lines and a radar antenna is pulled along the line to complete a GPR record (Grid Site 4).

Casa Grande Ruins National Monument occupies an approximate 480 acre site just north of Coolidge, in

western Pinal County, Arizona. Most of the site is in native range and consists mainly of creosote bush, cacti, mesquite, annual weeds and grasses. A majority of survey sites are located within a delineation of Coolidge sandy loam (soil map unit 11; <http://websoilsurvey.nrcs.usda.gov/app/>). The very deep, well drained Coolidge soil formed in alluvium. Typically, Coolidge soil has a calcic horizon within depths of 14 to 40 inches (<http://soildatamart.nrcs.usda.gov/>). The surface layer contains about 5 to 10 % clay. The clay content of the subsoil ranges from 20 to 30 %. In the subsoil, salinity and SAR (sodium absorption ratio) can range from 0 to 4 mmhos/cm and from 0 to 13, respectively. In the substratum, salinity and SAR can range from 4 to 8 mmhos/cm and from 13 to 40, respectively. Because of the presence of soluble salts, Coolidge soil is considered generally unsuited to deep exploration with GPR.

The portion of Compound IX, which was surveyed with EMI, consists of delineations of Coolidge sandy loam (soil map unit 11) and Laveen loam (soil map unit 28). The very deep, well drained Laveen soils formed in alluvium. Laveen soil is similar, but contains slightly more clay than Coolidge soil. Table 1 lists the taxonomic classifications of these soils.

Table 1. Taxonomic Classifications of Soil Mapped at Casa Grande Ruins National Monument

Soil Series	Taxonomic classification
Coolidge	Coarse-loamy, mixed, superactive, hyperthermic Typic Haplocalcids
Laveen	Coarse-loamy, mixed, superactive, hyperthermic Typic Haplocalcids

Survey Sites:

All grid sites located in Compound A were significantly compacted by pedestrian foot traffic. The grid site located within Compound C was less disturbed and trafficked. Figure 2 shows the locations of all GPR grids and transect sites within Casa Grande Ruins National Monument. Also shown in this figure are the locations of known, buried and exposed structural walls.

Grid Sites 1 & 2:

This site represents the largest grid area that was surveyed with GPR. This grid site was located along the southern margin of Compound A (in Figure 2, lower-right inset, the corners to Grid Site 1 are identified by blue dots). The dimensions of Grid Site 1 were 46 m (east-west) by 40 m (north-south). The origin of Grid Site 1 was located in the northwest corner. Radar traverse lines were spaced at 50 cm intervals and orientated in a north-south direction. Moving from west to east across Grid Site 1, a total of 93, 40-m traverses were completed with the 400 MHz antenna.

Grid Site 2 was located within Grid Site 1. The dimensions of Grid Site 2 were 40 m (east-west) by 40 m (north-south). The origin was located in the southwest corner of the grid. Grid 2 was established 1.5 m within the eastern and western boundaries of Grid Site 1. Radar traverse lines were spaced at 50 cm intervals and orientated in an east-west direction. Moving from south to north across Grid Site 2, a total of 81, 40-m traverses were completed with the 400 MHz antenna.

Grid Site 3:

This grid site was located a short distance to the south of *Casa Grande* in Compound A (in Figure 2, lower-right inset, the corners to Grid Site 3 are identified by grey dots). The dimensions of Grid Site 3 were 6 m (east-west) by 4 m (north-south). The origin was located in the northwest corner of the grid. Radar traverse lines were spaced at 25 cm intervals and orientated in a north-south direction. Moving from west to east across Grid Site 3, a total of 25, 4-m traverses were completed with the 400 MHz antenna.

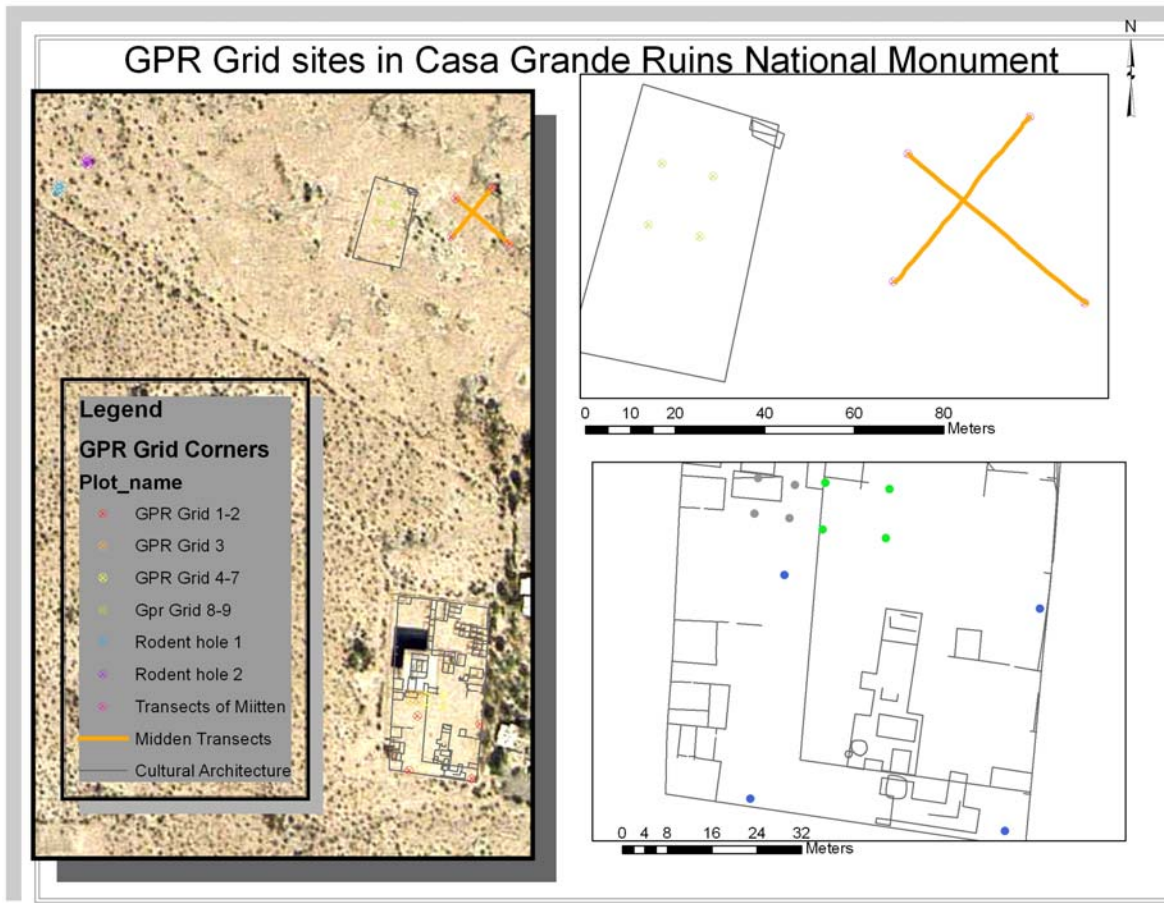


Figure 2. Locations of the various GPR grid and transect sites within Casa Grande Ruins National Monument. Image was prepared by Eric Drummond (GIS Analysis, USDI-NPS-IRGR, Lakewood, CO).

Grid Sites 4 thru 7:

This grid site was located immediately southeast of *Casa Grande* in Compound A (in Figure 2, lower-right inset, the corners to Grid Sites 4 thru 7 are identified by green dots). The dimensions of the grid were 10 m (east-west) by 10 m (north-south). Four separate surveys were conducted at this site: two with the 400 MHz antenna and two with the 200 MHz antenna. Surveys were conducted under both dry and moist (sprinkler irrigation was applied to the site) conditions to determine whether variations in soil moisture contents would improve the detection of buried structural walls. For the 400 MHz antenna, radar traverse lines were spaced at 25 cm intervals and orientated in a north-south direction. The origins of the grid were located in the northwest corner for the survey conducted under dry conditions and in the southeast corner for the survey conducted under wet conditions. Moving from west to east (Dry - Survey 4) and from east to west (Moist-Survey 5) across the grid site, a total of 41, 10-m traverses were completed with the 400 MHz antenna in each survey.

For the 200 MHz antenna, both surveys were conducted under moist conditions. For Survey 6, radar traverse lines were spaced at 50 cm intervals and orientated in a north-south direction. The origin was located in the southeast corner of the grid. Moving in a back and forth manner, in an east to west direction across the grid site, a total of 21, 10-m traverses were completed with the 200 MHz antenna (Survey 6). For Survey 7, radar traverse lines were spaced at 100 cm intervals and orientated in an east-west direction. The origin of this grid (Survey 7) was in the southeast corner. Moving in a south to north direction across the grid site, a total of 13, 10-m traverses were completed with the 200 MHz antenna (Survey 7).

Grid Sites 8 and 9:

This grid site was located in Compound C, a short distance to the northwest of *Casa Grande* and Compound A

(in Figure 2, left and upper right insets show the locations of Compound C and GPR midden transect lines). This grid site represents a relatively undisturbed and less trafficked area. The dimensions of Grid Sites 8 and 9 were 12 m (east-west) by 12 m (north-south). The origin of both grids was located in the southeast corner. Two surveys were conducted at this site: one with a 400 MHz antenna (Survey 8) and one with a 200 MHz antenna (Survey 9). For the 400 MHz antenna, radar traverse lines were spaced at 25 cm intervals and orientated in a north-south direction. Moving across the grid site from east to west, a total of 49, 12-m traverses were completed with the 400 MHz antenna (Survey 8). For the 200 MHz antenna, radar traverse lines were spaced at 50 cm intervals and orientated in a north-south direction. Moving across the grid site from east to west, a total of 25, 12-m traverses were completed with the 200 MHz antenna (Survey 9).



Figure 3. A low midden at Casa Grande Ruins National Monument.

Midden Transects:

Oval shaped mounds of less than 1 m height occur within Casa Grande Ruins National Monument. Typically, these mounds occur in clusters and are easily identifiable by their topographic expression and relief. These mounds have concentration of ceramics on the surface (see Figure 3) and are middens.

Two radar traverse lines were established across a low midden near Compound C (see Figure 2). In Figure 2, the location of these traverse lines are indicated by the two intersecting, orange-colored lines (see left and upper-right insets). The lines were 48 and 51 m long. Along each traverse line survey flags were inserted in the ground at 3-m intervals and served as reference or observation points. GPR surveys were completed along each line using both the 200 and 400 MHz antennas

Round-tailed Ground Squirrel Borrow Grids 1 and 2:

Ground-penetrating radar was used to map borrows of round-tailed ground squirrels. Two grid sites were located near the western boundary of Casa Grande Ruins National Monument (in Figure 2, left inset, approximate locations of the two grid sites are identified by blue- and pink-colored circles in the upper left-hand corner). The dimensions of these grids were 4 m (east-west) by 4 m (north-south). The origin was located in the southeast corner of each grid. Radar traverse lines were spaced at 25 cm intervals and orientated in a north-south direction. At each grid site, moving from east to west, a total of 17, 4-m traverses were completed with

the 400 MHz antenna.



Figure 4. A round-tailed ground squirrel at Casa Grande Ruins National Monument.

EMI Surveys:

EMI surveys were conducted across portions of Compounds C and IX (areas not shown in Figure 2). Spatial EC_a patterns were used to reveal the locations and general shapes of several middens.

Principals of Operation:

Ground-Penetrating Radar:

Ground-penetrating radar is an impulse radar system that has been specially designed for shallow, subsurface investigations. This system operates by transmitting short pulses of very high and ultra high frequency electromagnetic energy into the ground from an antenna. Each pulse consists of a spectrum of frequencies distributed around the center frequency of the transmitting antenna. Whenever a pulse contacts an interface separating layers of different dielectric permittivity (E_r), a portion of the energy is reflected back to a receiving antenna. The receiving unit amplifies and samples the reflected energy and converts it into a similarly shaped waveform in a lower frequency range. The processed reflected waveforms are displayed on a video screen and stored on a hard disk for future playback, processing, and/or printing.

Compared with other geophysical techniques, GPR provides high resolution images of the subsurface. The effective use of GPR is highly site specific and is interpreter dependent. Ground-penetrating radar does not work equally well in all soils. Soils having high electrical conductivity rapidly dissipate the radar's energy, restrict penetration depths, and create low signal to noise ratios, which impair image quality and interpretability. The performance of GPR is dependent upon the electrical conductivity of soils. In highly conductive soils, the use of GPR is inappropriate. Use of GPR has been most successful in areas of sandy or coarse-loamy soils. Generally, observation depths range from 5 to 30 m in sandy soils, 1 to 5 m in loamy soils, and less than 0.6 m in clayey soils.

GPR measures the time that is required for electromagnetic energy to travel from an antenna to an interface (i.e.,

soil horizon, stratigraphic layer, buried artifact) and back. The two-way travel time is a function of the velocity of signal propagation (v), which is inversely proportional to relative dielectric permittivity as shown in Equation [1] (Daniels, 2004):

$$\sqrt{E_r} = c/v \quad [1]$$

where c represents the velocity of light in a vacuum (0.2998 m/ns). E_r can range from 1 (air) to 80 (water). The relationship between depth (d), two-way travel time (t) and velocity of propagation (v), is shown in Equation [2] (Daniels, 2004):

$$d = vt/2 \quad [2]$$

Based on a known depth to a buried reflector, calculated values of E_r (for the upper 1 m of the soil) ranged from about 3.3 with the 200 MHz antenna to 4.5 with the 400 MHz antenna. Accordingly, dielectric permittivities of 3.3 and 4.5 were used in this study, yielding propagation velocities (v) of 0.141 and 0.164 m/ns, respectively. However, considerable spatial variability in soil material and compaction exists within each site. As this spatial variability introduces errors into depth calculations, depth estimates are regarded as close approximations.

Electromagnetic induction:

Electromagnetic induction uses electromagnetic energy to measure the apparent conductivity (EC_a) of earthen materials. Apparent conductivity is a weighted, average conductivity measurement for a column of earthen materials to a specific depth (Greenhouse and Slaine, 1983). Variations in EC_a are caused by changes in the electrical conductivity of earthen materials. The electrical conductivity of soils is influenced by the type and concentration of ions in solution, the amount and type of clays in the soil matrix, the volumetric water content, and the temperature and phase of the soil water (McNeill, 1980). The EC_a of soils increases with increases in soluble salts, water, and/or clay contents (Kachanoski et al., 1988; Rhoades et al., 1976).

Electromagnetic induction typically employs an instrument referred to as a ground conductivity meter. An alternating electrical current is passed through one of two small electric wire coils spaced a set distance apart and housed within the meter. The transmitter coil generates a time-varying electromagnetic field above the surface, inducing eddy currents to flow in the soil. These currents create a secondary magnetic field that propagates through the ground. The amplitude and phase components of this field are measured by the receiver coil. The secondary field is proportional to the ground current and is used to calculate an “*apparent*” value for soil electrical conductivity. The depth of penetration is dependent on the intercoil spacing, coil orientation, and frequency. Lateral resolution is equal to the coil spacing. An advantage of EMI methods is the fact that direct contact with the ground is unnecessary, and therefore the method can be used to rapidly acquire measurements of the near surface conductivity.

Results:

Grid Site 1:

Figure 5 is a portion of the radar record that was collected along the first 12.5 m of the Y = 40-m traverse line in Grid Site 1. This radar record has been migrated to compress hyperbolas and reduce diffraction tails caused by point reflectors. A horizontal high pass filter has been used to remove system noise. On the portion of the radar record shown in Figure 5, a high amplitude point reflector is evident to the immediate left of “A,” at a depth of about 50 cm. A second point reflector is evident below and slightly offset to the right of reflector “A” at a depth of about 75 cm. The multiple ringing of this reflector suggests a metallic object. These two subsurface reflectors are presumed to represent modern cultural features associated with the site of a former Park Superintendent’s residence. These reflectors help to confirm that the 400 MHz antenna can profile to a depth of at least 75 cm and can detect contrasting features in areas of Coolidge soil.

Also evident on the radar record shown in Figure 5, are a weakly contrasting subsurface feature to the left of “B” and an area of less contrasting (dense) surface soil materials around “C.” Difference in density and compaction between buried and partially buried caliche walls and enveloping soil materials were expected to be

manifested on radar records. These features (B and C in Figure 5), while not highly contrasting and noticeable, could represent the expression of buried caliche walls. If so, these features are difficult to discern and identify on 2D radar records.

The ground within Compound A is highly compacted. This compaction would reduce density and moisture differences between the caliche walls and the heavily foot trafficked soil materials. As a consequence, in areas of compacted surface soil materials, buried walls would be poorly manifested and difficult to discern on 2D radar records. Similar experiences are reported by Conyers and Cameron (1998) for a prehistoric Chacoan road in Utah.

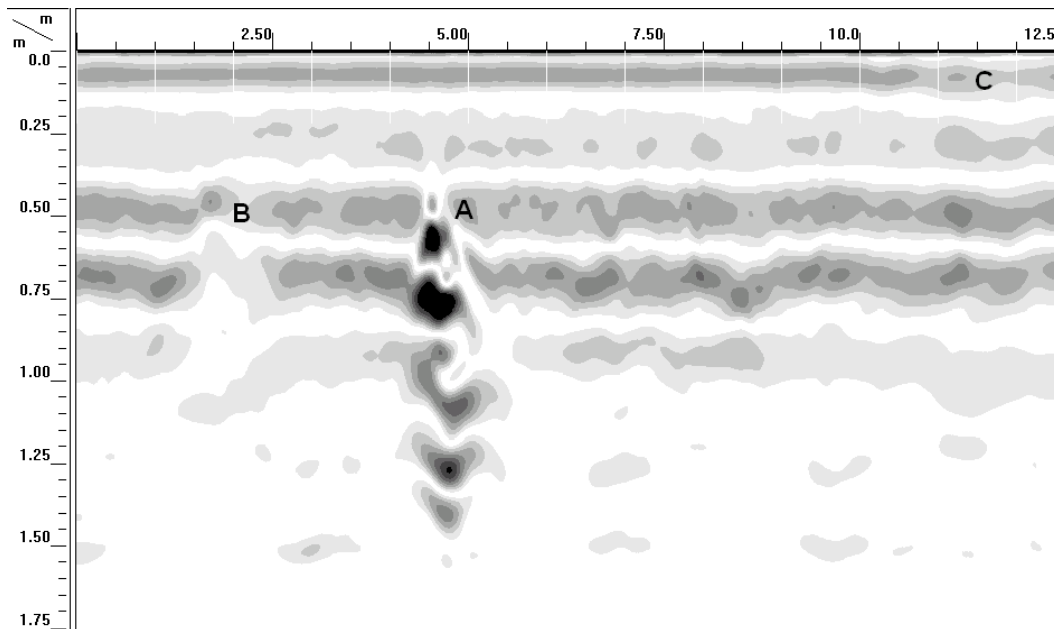


Figure 5. A representative portion of a radar record from Grid A (Line X = 40 m) showing both strongly (A) and weakly (B) expressed point reflectors and an area of contrasting surface soil materials (C).

The 2D radar records from this grid site revealed numerous subsurface reflectors that varied in size, depth, and reflected signal amplitudes. Most of these reflectors undoubtedly represented buried cultural features, and some possibly represent structural walls associated with the Hohokam culture. However, without intensive exploratory excavations, the identities of these objects remain unclear.

Figure 6 contains two sets (upper and lower) of time-sliced images from Grid Site 1. The two set of plots are for different depths with each set containing two identical plots (one annotated the other not). In Figure 6, the plots on the right have been annotated. These 3D cube images are considered pseudo-sections of the grid area as the vertical scale merely approximates the depth of subsurface features. The upper two plots are horizontal time-slice images made at the 50 cm soil depth. The lower two plots are horizontal time-slice images made at the 100 cm soil depth. The thickness of each slice is about 32 cm. In each plot, north is to the left. To create these images, the maximum reflected wave amplitude method was used. Depths are based on a constant propagation velocity of 0.141 m/ns.

In an attempt to detect subtle subsurface features, the radar data set from this grid site was submitted to Hilbert magnitude transformations (both phase and frequency information) and spatial filtration, but to no avail. The use of these processing techniques did not enhance the imaging of subtle features nor improved interpretations. The plots shown in Figure 6 have been subjected to very little processing and have not been migrated.

In the plots shown in Figure 6, along most of the southern boundary (right-hand plot margin) of this site, a comparatively distinct zone has been enclosed by a green-colored rectangle. This zone appears to contain relatively few subsurface reflectors and is therefore assumed to consist of fairly homogenous materials. This fairly homogenous and unremarkable zone has been identified with the letter “A.” This area is noticeable in both the 50 and 100 cm depth-sliced images. It appears to extend across the southern portion of the grid from about Y = 8 m to Y = 46 m, and from X = 31 and 32 m, to X = 40 m. This represents a likely area for habitation and buried structural elements. While nothing exceptional is evident in this zone, and perhaps a stretch of the imagination, a “wall-like” feature appears to extend in an east to west (from top to bottom of plots) direction along its northern border (X = 31 to 32 m).

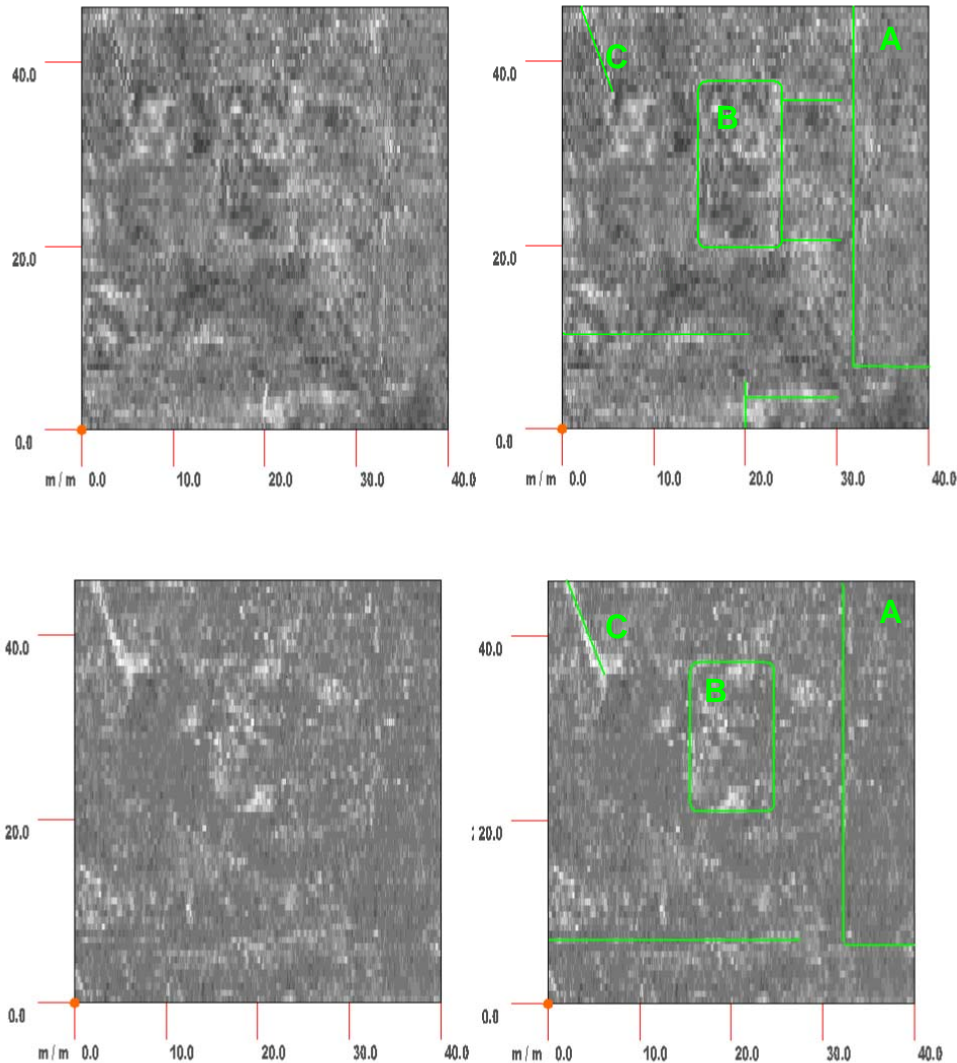


Figure 6. Two sets of time-sliced images from Grid Site 1, Compound A. Horizontal time-slice images for depths of 50 cm (upper plots) and 100 cm (lower plots). The thickness of each slice is 32 cm. In each plot, North is to the left.

Additional features, believed to be associated with the site of the former residence, have been enclosed in a green-colored rectangle, which has been identified with the letter “B”. This area contains a collage of both high and low amplitude reflections that are believed to represent modern artifacts. Also apparent in these plots is a conspicuous, high-amplitude, linear feature, “C”, that is located in the northeast corner of the grid area. This

linear feature extends in a southwesterly direction towards the site of the former residence and may represent a buried utility or drain line. Other linear features have been identified in the upper and lower, right-hand plots with green-colored lines. As none of these features appear to persist with depth, it is unlikely that they represent buried walls.

Grid Site 2:

This slightly smaller survey area was located within Grid Site 1. Radar traverses were conducted in an east to west direction, which is orthogonal to the direction conducted in the survey of Grid Site 1. As the orientation of buried structural features and archaeological remains is unpredictable, two GPR surveys of a site in orthogonal directions are often recommended (Lualdi et al., 2006; Dabas et al., 2000). However, this places additional demands on resources and greater burdens on the positional accuracy of the two radar data sets. The positional accuracy achieved in the surveys of Grid Sites 1 & 2 was too poor to combine the separate data sets into one final 3D representation.

The radar data from the survey of Grid Site 2 were comparable to the data collected from the survey of Grid Site 1 and did not provide any additional information on the location and identification of buried structural walls within the compound. As a consequence, the data will not be discussed further.

Grid Site 3:

This very small grid site contained an exposed buried wall (see Figure 7), which was profiled with GPR. Knowing the location of the wall, conducting radar traverses at very slow speeds of advance, and the use of signal processing techniques greatly improved the recognition of this feature on radar records. However, even with these measures the partially exposed, buried wall was not evident on all radar records.



Figure 7. The top of a partially-exposed, buried wall (see light-colored linear feature in foreground) is evident on this photograph of Grid Site 3.

In Figure 8, a range-gained and color-enhanced radar record clearly shows the location of the partially-exposed, buried wall. In Figure 8, the wall is located between the 1 and 2 m distance marks. This feature was not initially evident on the processed radar record. Color transformations, color table and range gain adjustments were needed to “bring out” this feature on this radar record. Though repeatedly passed over with the 400 MHz antenna, even with these display and processing options, the low amplitude and unremarkable reflective characteristics of this partially-exposed, buried wall made it indistinguishable on many of the radar records. In areas of compacted soil materials, such as founded in the heavily foot trafficked areas of Compound A, caliche

walls are very difficult to distinguish on radar records.

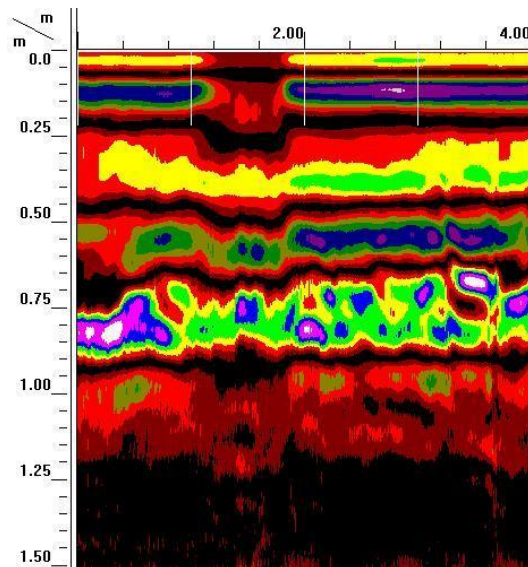


Figure 8. The disruption of surface and near-surface reflections and the faint indentation on this radar record indicates the location of the partially-exposed, buried wall in Grid Site 3.

Grid Site 4 thru 7:

Conyer and Cameron (1998) reported that the floors of pit structures visible on radar records under dry conditions were not evident under wet conditions. Unwanted, high amplitude reflections, which were caused by pockets of soil materials with higher water contents, masked the floors on radar records. In general, masonry that is dry, homogenous and in good condition has been found to provide more favorable radar targets than masonry that is inhomogeneous, rubble, or with higher conductivity (Colla and Maierhofer, 2000). In addition, differences in moisture content and signal velocity have been used with GPR to map zones of potential archaeological interest (Pipan et al., 1999).

Figure 8 shows different time-slice images of the grid area. Each plot represents a pseudo-image of the radar data collected at this grid site with the 400 MHz antenna. The two upper plots are identical time-sliced maps that were collected under dry conditions. The slice is 0.34 m thick and was made at a depth of 50 cm. The upper right-hand plot has been underscored with line segments representing buried utility lines and potential structural walls. In each plot, the location of a modern utility line that bisects the site from east to west is clearly expressed by a high amplitude linear reflector that occurs at approximately $X = 5.3$ m. This feature has been highlighted with a solid, black line in the upper right-hand plot. Overlying this feature, the backfilled soil materials were noticeably less dense than the adjoining less disturbed, but more highly compacted soil materials. In the upper plots of Figure 8, a very faint, linear reflection pattern extends across the site from southwest to northeast. This feature has been emphasized with a segmented, black line in the upper right-hand plot. In the upper right-hand corner of the upper plots, spatial signal amplitude patterns suggest the presence of buried wall structures. Though the reflections are rather indistinct and blurred, the locations of possible buried walls have been indicated in the upper right-hand plot.

The lower two plots represent pseudo images of the radar data, which were collected with the 400 MHz antenna under moist conditions (a sprinkler was run across the site for several hours). These time-slice images are 0.34 m thick and represent horizontal slices made at depths of 0.00 (lower, left-hand plot) and 0.50 m (lower, right-hand plot). In each plot, the location of a modern utility line that bisects the site from east to west is clearly expressed by a linear pattern of high amplitude reflections that occurs at approximately $X = 4.8$ m. The

difference in the location of this feature on the plots of the two surveys (see upper and lower plots in Figure 8) is attributed to antenna offset caused by conducting the radar traverses on different sides of the survey flags.

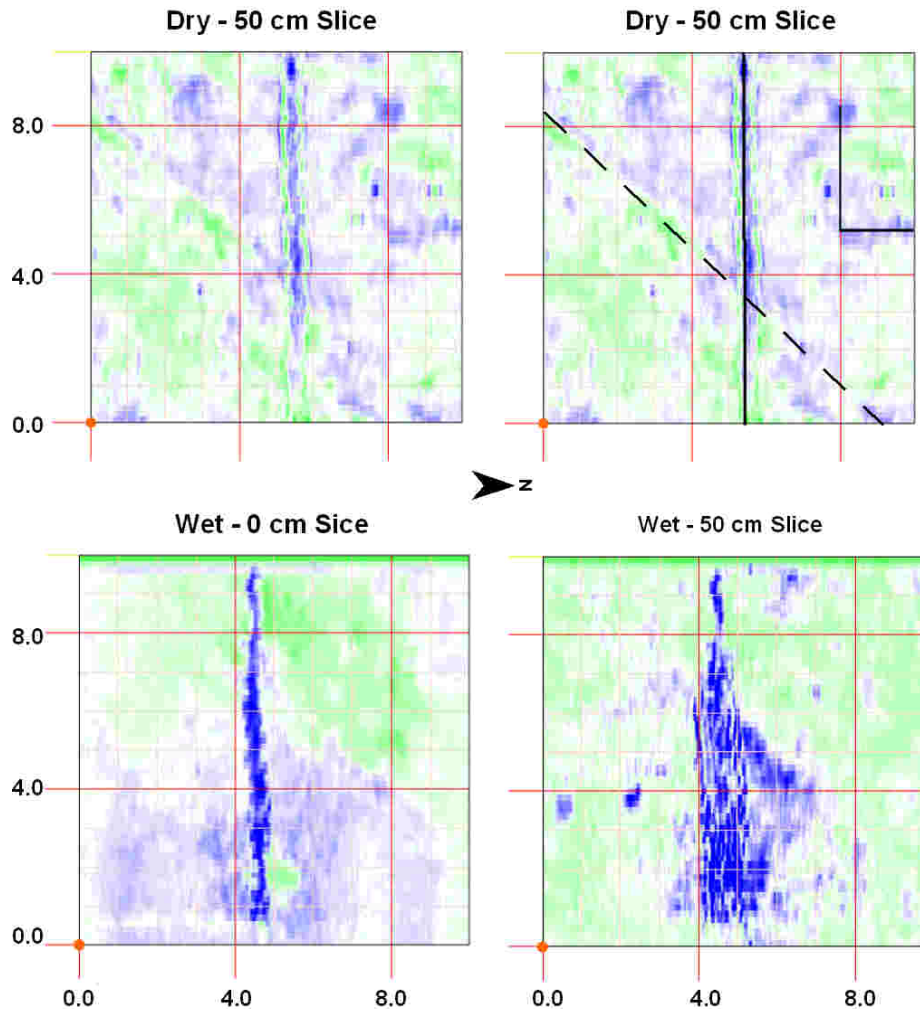


Figure 8. Time-sliced images collected with the 400 MHz antenna from Grid Site 4 (upper plots) under dry conditions and Grid Site 5 (lower plots) under moist conditions.

The recently buried utility line is more pronounced in the lower plots of Figure 8. The soil materials overlying this refilled trench are less compacted, more permeable, and have higher water content than adjoining soil materials. While the wetted area is discernible in the lower plots, the structural features inferred in the upper plots have been obscured by the addition of water. In areas of compacted soil materials, buried, prehistoric caliche walls of the Hohokam culture are similar to surrounding soil materials and represent poor radar reflectors. Conducting surveys under wetter soil conditions masked what little evidence there was of these structures on radar records.

Grid Sites 8 and 9:

Compound C represents a relatively undisturbed and less trafficked area. Two surveys (one with the 400 MHz and one with the 200 MHz antennas) were conducted on what appeared to be a central courtyard in an attempt to locate buried structural walls. As with the other grid sites, the depth of penetration of the 200 and 400 MHz antennas were comparable. Because the resolution of the 400 MHz antenna was superior to that of the 200 MHz antenna, the 400 MHz continued to be the antenna of choice.

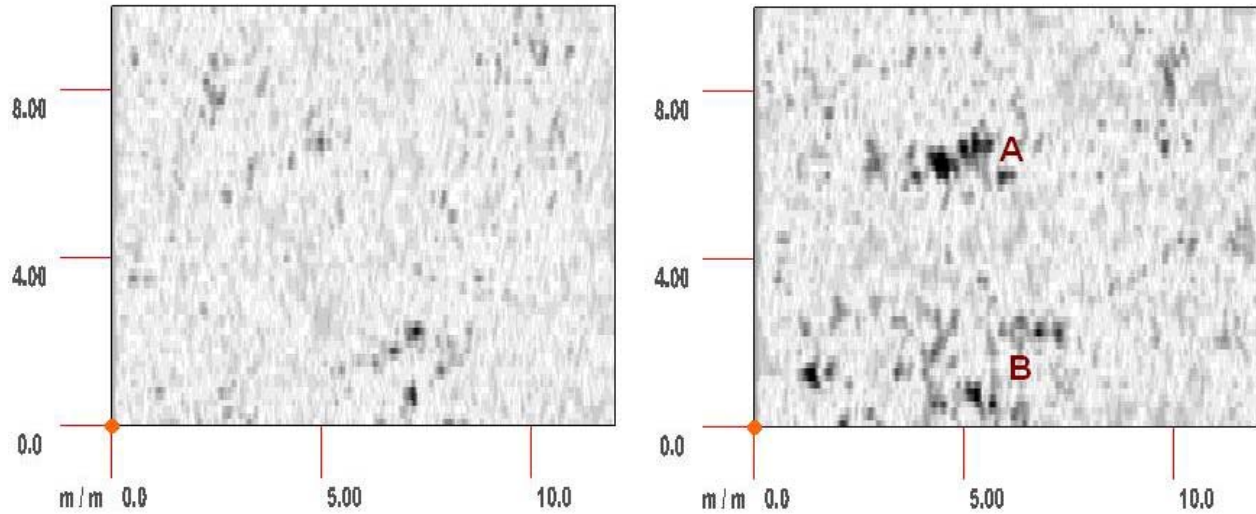


Figure 9. Time-sliced images collected with the 400 MHz antenna from Compound C. Horizontal time-slice images for depths of 50 cm (right-hand plot) and 100 cm (left-hand plot). The thickness of each slice is 32 cm. In each plot, North is to the left.

Figure 9 contains two time-slice images of the radar data collected with the 400 Hz antenna at the grid site. These time-slice images are 0.32 m thick and were made at depths of 50 (left-hand plot) and 100 cm (right-hand plot). These plots are relatively unremarkable, with no well-defined linear features. These plots contain few persistent, higher amplitude reflectors that could represent buried archaeological features. In the 100 cm depth slice image, two areas containing more depth-enduring, high amplitude reflections have been labeled “A” and “B”. These reflectors represent the most promising sites for buried artifacts and their appearances suggest possible wall structures.

At Grid Sites 8 and 9, if buried wall structures exist, these features are no more discernible in this setting than in the more trafficked and compacted soil setting found within Compound A.

Middens:

Middens contain waste products, which may accumulate for several generations under sedentary cultures. Middens are known to contain animal bones, shells, sherds, lithics and other artifacts. Most middens within Casa Grande Ruins National Monument form easily identifiable mounds whose surfaces are littered with sherds and lithics. Figure 10 is a portion of a radar record that was collected with the 400 MHz antenna over a midden mound. The radar record shown in Figure 10 has been *terrain corrected* based on rough calculation of the elevation at each of the equally spaced (3 m) reference marks. *Terrain correction* or *surface normalization* corrects the radar record for changes in elevation and, in this example, improves interpretations and the association of subsurface reflectors with the midden mound. Across the midden, the 400 MHz antenna provided a penetration depth of about 1.0 m. Within the midden mound, a larger number of higher-amplitude point reflectors are evident and suggest concentrations of buried artifacts (see Figure 10).

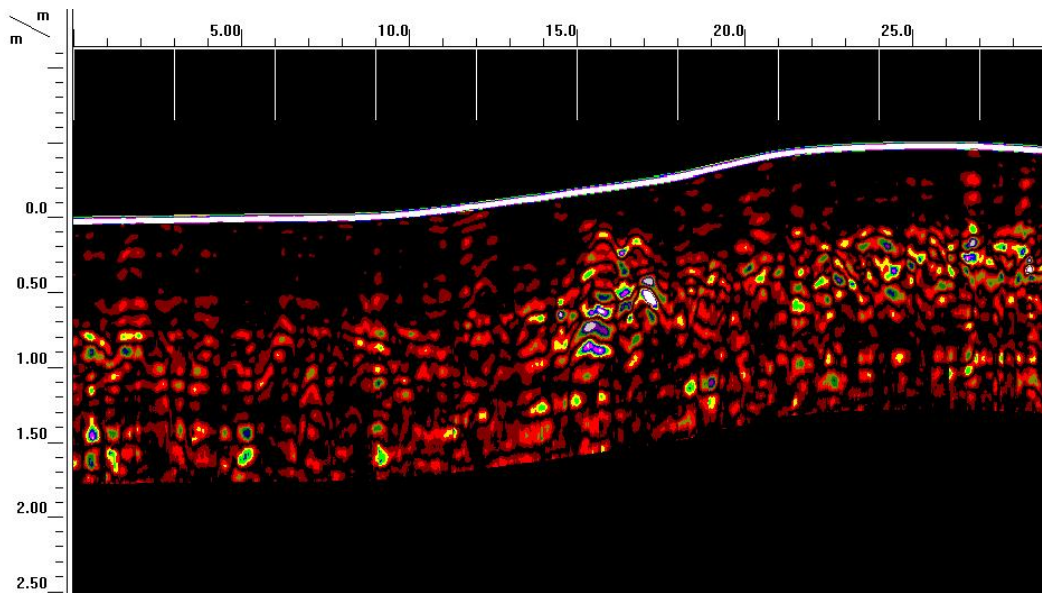


Figure 10. A greater concentration of point reflectors is evident beneath a midden.

Electromagnetic induction has been used to locate and identify large earthen features, mounds and middens (Bevan, 1983). Typically, compared with the surrounding soils, middens have higher EC_a . In many instances, middens are noticeable by their relief, geometry, surface soil coloration and scattered cultural debris, and therefore geophysical tools are unnecessary for locating and identifying these features. However, in some areas, middens have been leveled or are not clearly expressed. In these instances, EMI offers a rapid means to reconnoiter fairly large areas for the presences of these archaeological features.

Table 2. Basic statistics for the EMI surveys that were conducted across portions of two compounds within Casa Grande Ruins National Monument.

<i>Site</i>	<i>Observations</i>	<i>Minimum</i>	<i>25% tile</i>	<i>75% tile</i>	<i>Maximum</i>	<i>Average</i>	<i>Standard Deviation</i>
Compound C	2515	-10.25	5.25	9.38	21.13	7.57	3.24
Compound IX	4265	-17.88	4.13	7.63	23.25	6.53	3.71

Electromagnetic surveys were conducted with an EM38 meter (operated in the vertical dipole orientation) over portions of Compounds C and IX. Basic statistics for these EMI surveys are provided in Table 2. Within the surveyed portion of Compound C, EC_a averaged 7.57 mS/m and ranged from about -10.2 to 21.1 mS/m. One-half of the EC_a measurements were between about 5.2 and 9.4 mS/m. Within the surveyed portion of Compound IX, EC_a averaged 6.53 mS/m and ranged from about -17.8 to 23.2 mS/m. One-half of the EC_a measurements were between about 4.1 and 7.6 mS/m. Negative measurements are attributed to the presence of metallic artifacts. The comparatively low EC_a across most of these compounds is attributed to the low clay, moisture, and soluble salt contents of the Coolidge soil.

Intrinsic changes in EC_a have been associated with “*cultural loading*” and have served as fingerprints for determining whether mounds are artificial or natural (Dalan and Bevan, 2002). In the present surveys, higher EC_a readings were obtained over the midden mounds. The higher conductivity over the midden is probably caused by the cultural debris within these mounds. Marine shells were an important trade and ornamental item for the Hohokam culture (Mitchell and Foster, 2000). Middens within Casa Grande Ruins National Monument could therefore contain high concentrations of calcium carbonate, which would partially explain their higher EC_a .

Figures 11 and 12 are plots of spatial EC_a patterns within portions of Compounds C and IX, respectively. Spatial EC_a patterns revealed the general shape and location of middens. In Figures 11 and 12, spatial EC_a patterns suggest that the mounds form an anastomosing network. The interconnected middens appear to surround core areas of lower EC_a . In general, in areas of undisturbed Coolidge and Laveen soils, EC_a is less than 8 mS/m. Midden mounds were found to have an EC_a greater than 8 mS/m. Relative differences in EC_a across the midden mounds may provide clues as to the type and concentration of artifacts and/or possibly shell fragments that are buried within these features.

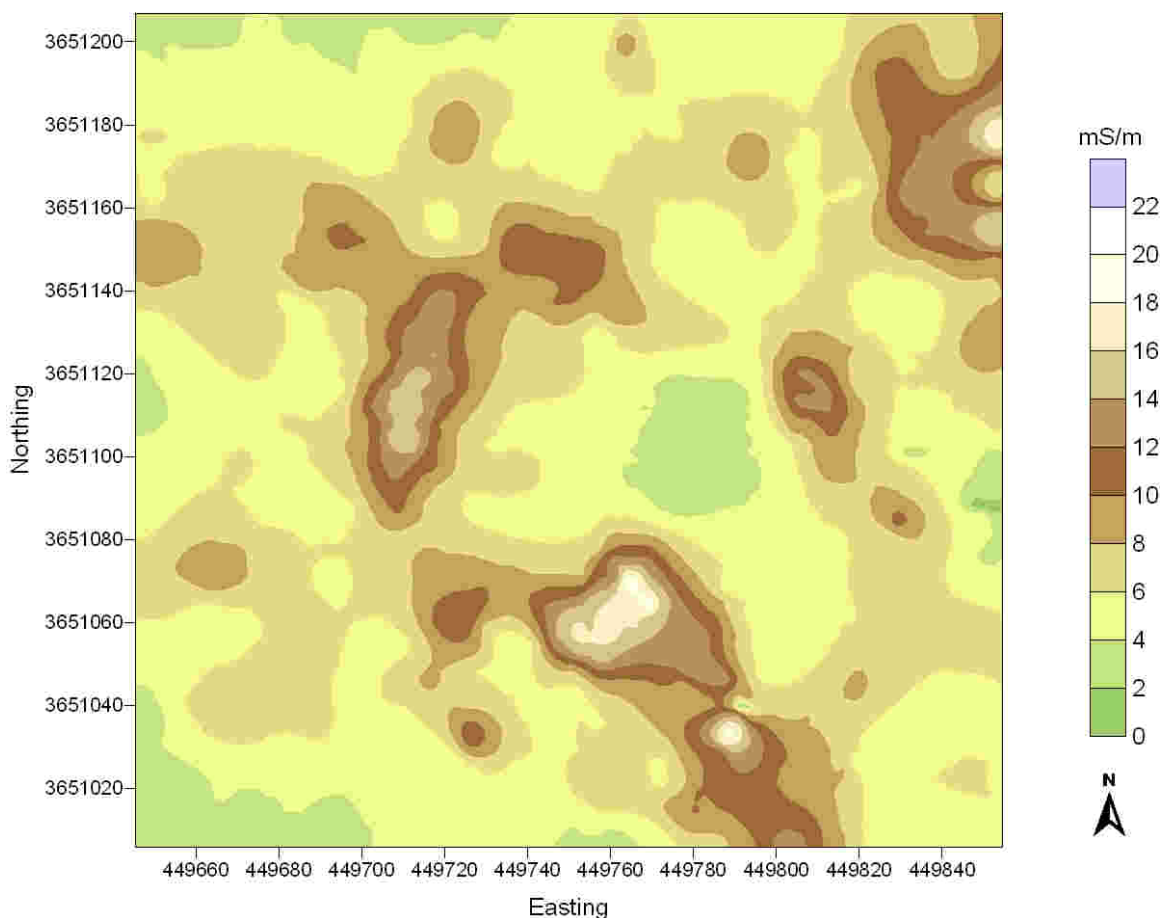


Figure 11. Spatial EC_a patterns across a portion of Compound C obtained with the EM38 meter operated in the vertical dipole orientation

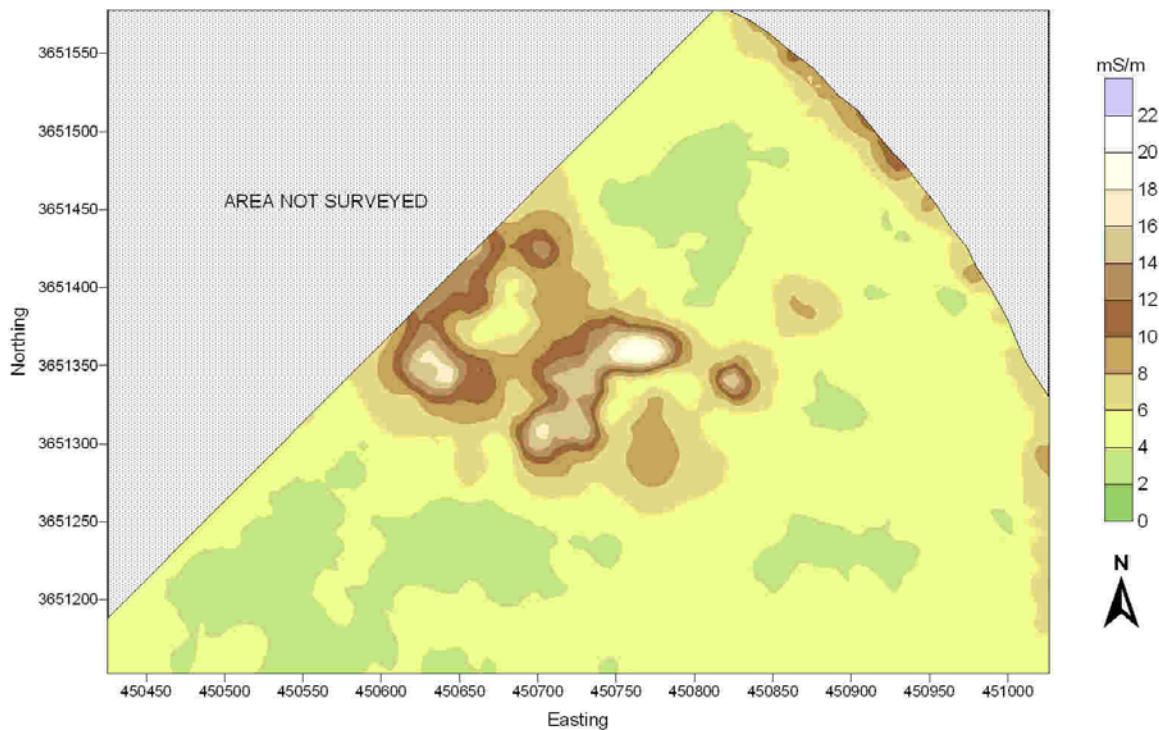


Figure 12. Spatial EC_a patterns across a portion of Compound IX obtained with the EM38 meter operated in the vertical dipole orientation

Round-tailed ground squirrel burrows:

The size and distribution of animal burrows is dependent on animal species, soil type, and plant communities. Ground-penetrating radar has been used to investigate the geometry of rabbit warrens (Stott, 1996) and badger setts (Nichol et al., 2003). Nichol et al. (2003) identified a 324-m badger tunnel network that ranged in depth from 0 to 2 m. In their study, high amplitude reflections were identified as air voids, which were associated with access tunnels and living chambers; low amplitude reflections were associated with a reduction in the air-void space caused by collapsed or abandonment of tunnels. Typically, badger tunnels measured 30 to 35 cm wide and 25 to 30 cm high.

Directed by Dr. T Karen Munroe, the use of GPR to map the burrows of round-tailed ground squirrels was explored at Casa Grande Ruins National Monument. The higher resolution of the 900 MHz antenna made it more suitable for investigating the ground-squirrel burrow networks. Unfortunately, the 900 MHz antenna malfunctioned and the lower frequency 400 MHz was used as a substitute. It is believed that the higher frequency 900 MHz antenna would have been a more appropriate antenna had it been available for testing.

Figure 13 shows two, pseudo-images of a 4 by 4-m grid area with horizontal time-slices at depths of 0.18 (upper plot) and 0.48 (lower plot) m. In each plot, the time-slice is 0.23 m thick. In each plot, burrows appear as higher-amplitude (darker-colored) reflections. Accordingly, burrows are concentrated in the northeast corner of the grid (confirmed by visual observations). Tunnels appear to vary in dimension and orientation. Using the *Movie* mode function of RADAN, the 3D image automatically scrolls through the time-slices allowing the geometry of the burrows to be more fully expressed and evident. Care must be exercised in distinguishing roots, rock fragments, and artifacts from burrow as each can provide similar reflections.

Figure 14 represents a high resolution, 3D transparency of Ground-Squirrel Grid Site 1. This display highlights the peak amplitudes and the locations of the squirrel burrows in a three-dimensional data cube. The general location, depth and geometry of the burrows are shown in this image.

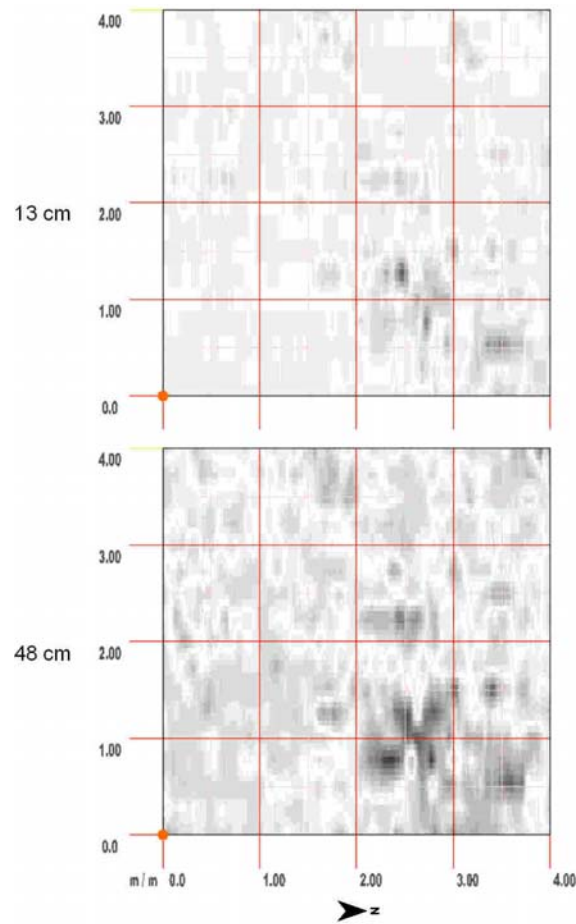


Figure 13. Time-sliced images collected with the 400 MHz antenna from the Round-tailed Ground Squirrel Grid 1. Horizontal time-slice images for depths of 18 cm (upper plot) and 48 cm (lower plot). The thickness of each slice is 23 cm. The maximum reflected wave amplitude method was used. A constant velocity of 0.141 m/ns was assumed.

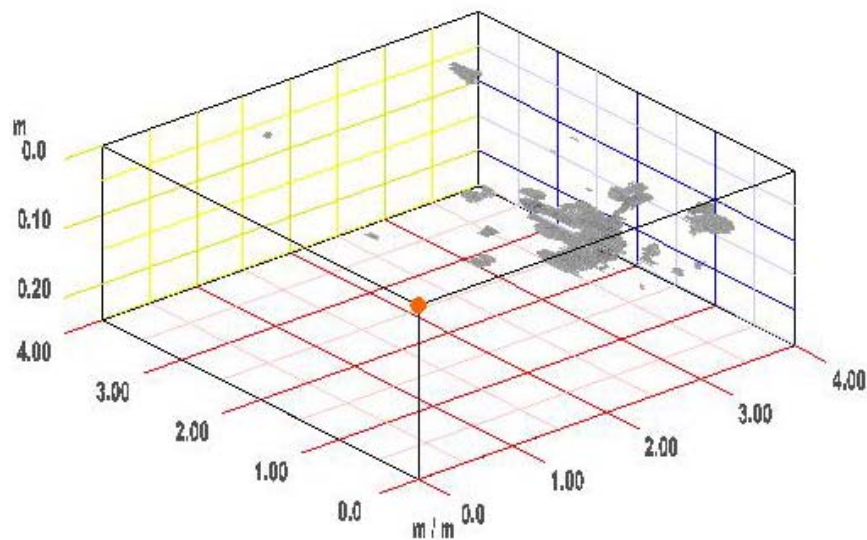


Figure 14. A 3D transparency view of the ground squirrel burrows beneath Ground-Squirrel Grid Site 1.

References:

- Baker, J. A., N. L. Anderson, and P. J. Pilles, 1997. Ground-penetrating radar surveying in support of archaeological site investigations. *Computers & Geosciences*, 23 (10): 1093-1099.
- Berard, B. A., and J-M. Maillol, 2007. Multi-offset ground-penetrating radar data for improved imaging in areas of lateral complexity – Application at a Native American site. *Journal of Applied Geophysics*.
- Bevan, B., 1983. Electromagnetics for mapping buried earth features. *Journal of Field Archaeology* 10: 47-54.
- Bevan, B., 2000. Resistivity pseudosections at Fort Lowell and Casa Grande. Technical Report. Geosight, Weems, Virginia.
- Bevan, B. W., D. G. Orr, and B. S. Blades, 1984. The discovery of the Taylor House at the Petersburg National Battlefield. *Historical Archaeology*, (18): 64-74.
- Colla, C., and Ch. Maierhofer, 2000. Investigation of historic masonry via radar reflection and tomography. 893-897 pp. IN: Noon, D. A., G. F. Stickley, and D. Longstaff (editors) *Proceedings of Eight International Conference on Ground-Penetrating Radar*, May 23 to 26, 2000, Goldcoast, Queensland, Australia. SPIE Vol. 4084.
- Conyers, L. B., 2006. Ground-penetrating radar techniques to discover and map historic graves. *Historical Archaeology* 40(3): 64-73.
- Conyers, L. B., and C. M. Cameron, 1998. Ground-penetrating radar techniques and three-dimensional computer mapping in the American Southwest. *Journal of Field Archaeology* 25: 417-430.
- Conyers, L. B., and D. Goodman, 1997. *Ground-Penetrating Radar; an introduction for archaeologists*. AltaMira Press, Walnut Creek, CA.
- Conyers, L. B., and R. Osburn, 2006. GPR mapping to test anthropological hypotheses: A study from Comb Wash, Utah, American Southwest. Paper ARC: 30_hbp. 1-4 pp. IN: Daniels, J. J., and C-C. Chen (Eds.) *Proceedings of the 11th International Conference on Ground Penetrating Radar*, Columbus, Ohio, June 19 – 22, 2006. CD.
- Dabas, M., C. Camerlynck, and P. Freixas i Camps, 2000. Simultaneous use of electrostatic quadrupole and GPR in urban context: Investigation of the basement of the Cathedral of Girona (Catalunya, Spain). *Geophysics*, 65(2): 526-532.
- Dalan, R. A., 1990. Defining archaeological features with electromagnetic surveys at the Cahokia Mounds State Historic Site. *Geophysics* 56(8): 1280-1287.
- Dalan, R. A., and B. W. Bevan, 2002. Geophysical indicators of culturally emplaced soils and sediments. *Geoarchaeology: An International Journal* 17(8): 779-810.
- Daniels D. J., 2004. *Ground Penetrating Radar; 2nd Edition*. The Institute of Electrical Engineers, London, United Kingdom.
- da Silva Cezar, G., P. L. F. da Rocha, A. Buarque, and A. da Costa, 2001. Two Brazilian archaeological sites investigated by GPR: Serrano and Morro Grande. *Journal of Applied Geophysics* 47: 227-240.
- Evangelista, R., P. Magee, and E. Wedepohl, 2002. 3D imaging of Iron Age archaeological site: GPR analysis at

- Muweilah, United Arab Emirates (UAE). 108-114 pp. IN: Koppenjan, S. K. and H. Lee (editors) Proceedings of Ninth International Conference on Ground-Penetrating Radar, 30 April to 2 May 2002. Santa Barbara, CA. SPIE Vol. 4758.
- Frohlich, B., and W. J. Lancaster, 1986. Electromagnetic surveying in current Middle Eastern archaeology: Application and evaluation. *Geophysics* 51(7):1414-1425.
- Geonics Limited, 1998. EM38 ground conductivity meter operating manual. Geonics Ltd., Mississauga, Ontario.
- Greenhouse, J. P., and D. D. Slaine, 1983. The use of reconnaissance electromagnetic methods to map contaminant migration. *Ground Water Monitoring Review* 3(2): 47-59.
- Imai, T., T. Sakayama, and T. Kanemori, 1987. Use of ground-probing radar and resistivity surveys for archaeological investigations. *Geophysics* 52(2): 137-150.
- Jol, H. M., R. J. DeChaine, and R. Eisenman, 2002. Archaeological GPR investigation at Rennes-le-Château, France. 91 -95 pp. IN: Koppenjan, S. K. and H. Lee (editors) Proceedings of Ninth International Conference on Ground-Penetrating Radar, 30 April to 2 May 2002. Santa Barbara, CA. SPIE Vol. 4758.
- Kachanoski, R. G., E. G. Gregorich, and I. J. Van Wesenbeeck, 1988. Estimating spatial variations of soil water content using noncontacting electromagnetic inductive methods. *Can. J. Soil Sci.* 68:715-722.
- Leckebusch, J., 2000. Two- and three-dimensional ground-penetrating radar surveys across a medieval choir: a case study in archaeology. *Archaeological Prospection*, 7: 189-200.
- Lualdi, M., L. Zanzi, and G. Sosio, 2006. A 3D GPR survey methodology for archaeological applications. Paper ARC: 166_spj. 1-9 pp. IN: Daniels, J. J., and C-C. Chen (Eds.) Proceedings of the 11th International Conference on Ground Penetrating Radar, Columbus, Ohio, June 19 – 22, 2006. CD.
- Lucius, J. E., and M. H. Powers, 1997. Multi-frequency GPR Surveys. 355-364 pp. IN: Proceedings of the Symposium on the Application of Geophysics to Engineering and Environmental Problems, March 23-26, 1997, Reno, Nevada. Environmental and Engineering Geophysical Society, Wheat Ridge, Colorado.
- McNeill, J. D., 1980. Electrical Conductivity of soils and rocks. Technical Note TN-5. Geonics Ltd., Mississauga, Ontario.
- Mitchell, D. R., and M. S. Foster, 2000. Hohokam shell middens along the Sea of Cortez, Puerto Peñasco, Sonora, Mexico. *Journal of Field Archaeology* 27: 27-41.
- Moorman, B. J., J.-M. Maillol, J. L. Williams, F. S. Walter, and W. D. Glanzman, 2002. Imaging the past: Archaeological radar stratigraphic analysis at Mahram Bilqis. 96 -101 pp. IN: Koppenjan, S. K. and H. Lee (editors) Proceedings of Ninth International Conference on Ground-Penetrating Radar, 30 April to 2 May 2002. Santa Barbara, CA. SPIE Vol. 4758.
- Nichol, D., J. W. Lenham, and J. M. Reynolds, 2003. Application of ground-penetrating radar to investigate the effects of badger setts on slope stability at St Asaph Bypass, North Wales. *Quarterly Journal of Engineering Geology and Hydrogeology (UK)* 36(2): 143-153.
- Nobes, D. V., and B. Lintott, 2000. Rutherford's "Old Tin Shed": Mapping the foundations of a Victorian-age lecture hall. 887-892 pp. IN: Noon, D. A., G. F. Stickley, and D. Longstaff (editors) Proceedings of Eight International Conference on Ground-Penetrating Radar, May 23 to 26, 2000, Goldcoast, Queensland, Australia. SPIE Vol. 4084.

- Pérez Gracia, V., J. Antonio Canas, L. G. Pujades, J. Clapés, O. Caselles, F. García, and R. Osorio, 2000. GPR survey to confirm the location of ancient structures under the Valencian Cathedral (Spain). *Journal of Applied Geophysics* 48: 167-174.
- Pipan, M., L. Baradello, E. Forte, A. Prizzon, and I. Finetti, 1999. 2-D and 3-D processing and interpretation of multi-fold ground penetrating radar data: a case history from an archaeological site. *Journal of Applied Geophysics* 41: 271-292.
- Rhoades, J. D., P. A. Raats, and R. J. Prather, 1976. Effects of liquid-phase electrical conductivity, water content, and surface conductivity on bulk soil electrical conductivity. *Soil Sci. Soc. Am. J.* 40:651-655.
- Sambuelli, L., L. V. Socco, and L. Brecciaroli, 1999. Acquisition and processing of electric, magnetic and GPR data on a Roman site (Victimulae, Salussola, Biella). *Journal of Applied Geophysics*, 41: 189-204.
- Sternberg, B. K., and J. W. McGill, 1995. Archaeological studies in southern Arizona using ground-penetrating radar. *Journal of Applied Geophysics*, 33: 209-225.
- Stott, P., 1996. Ground-penetrating radar: a technique for investigating the burrow structure of fossorial vertebrates. *Wildlife Research* 2: 519-530.
- Utsi, E., 2006. Improving definition: GPR investigation at Westminster Abbey. Paper ARC: 83_fbr. 1-7 pp. IN: Daniels, J. J., and C-C. Chen (Eds.) *Proceedings of the 11th International Conference on Ground Penetrating Radar*, Columbus, Ohio, June 19 – 22, 2006. CD.
- Utsi, E. and A. Alani, 2002. Barcombe Roman Villa: An example in GPR time slicing and comparative geophysics. 102 -107 pp. IN: Koppenjan, S. K. and H. Lee (editors) *Proceedings of Ninth International Conference on Ground-Penetrating Radar*, 30 April to 2 May 2002. Santa Barbara, CA. SPIE Vol. 4758.
- Vickers, R., L. T. Dolphin, and D. Johnson, 1976. Archaeological investigations at Chaco Canyon using subsurface radar. 81-101 pp. IN: Lyons, T. R. (ed.) *Remote Sensing Experiments in Cultural Resource Studies at Chaco Canyon*. USDI-NPS and the University of New Mexico, Albuquerque, New Mexico.
- Whiting, B. M., D. P. McFarland, and S. Hackenberger, 2001a. Three-dimensional GPR study of a prehistoric site in Barbados, West Indies. *Journal of Applied Geophysics* 47: 217-226.
- Whiting, B. M. D., McFarland. D. P., and S. Hackenberger, 2001b. Preliminary results of three-dimensional GPR-based study of a prehistoric site in Barbados, West Indies. 260-267 pp. IN: (Noon, D. ed.) *Proceedings Eight International Conference on Ground-Penetrating Radar*. May 23 to 26, 2000, Goldcoast, Queensland, Australia. The University of Queensland.